Proceedings of the 21st ICSMGE, Vienna, Austria, 14 – 19 June 2026. Pistrol, Adam & Schweiger (eds.)
Published by: ÖGG, Austrian Society for Geomechanics, Salzburg, Austria, ISBN 978-3-9503898-4-5
https://doi.org/10.53243/ICSMGE2026-801

Insight into Pile Run Risk of Offshore Pile during Installation

Indrasenan Thusyanthan,
Aramco, Dhahran, Kingdom of Saudi Arabia. it206@cantab.net

Anastasios Batilas, Martin Gichura, David Champness
Venterra Group, United Kingdom

ABSTRACT: The offshore wind industry is developing at a rapid pace with large wind turbine generators. In order to support this fast growth of offshore wind farms, large-diameter monopiles are being installed in offshore regions where the industry has limited knowledge of installation experience and ground conditions. This has led to various installation challenges, and pile run is one of the key challenges. Pile run is when a pile undergoes sudden and uncontrolled freefall, which was not predicted. The pile run phenomenon is not well understood by the industry, and there is currently a lot of active research on this topic. Pile run causes a significant risk to the project schedule, cost and to the safety of the vessel and operational personnel. Hence, understanding the pile run risk at the early stages of a project is vital for the success of a project. This paper provides insight into all the factors that could contribute to a pile run incident and provides recommendations on how pile run risks can be better predicted. Key factors that could contribute to pile run are investigated, and a better method of pile run prediction is proposed based on numerical work. This paper also presents results from numerical analysis, which provide better insight into excess pore pressures generated during pile driving and how that could initiate pile run.

KEYWORDS: Pile run, prediction, Plaxis 2D, UBC3D-PLM model

1 INTRODUCTION

As the use of offshore wind energy expands globally, the industry continually enhances its ability to adapt to local conditions and demands, striving to provide more reliable and efficient solutions for large-scale energy generation (GWEC, 2025). This expansion requires installing larger monopile foundations in increasingly challenging offshore environments, often in areas with complex soil conditions. One of the most critical installation challenges facing the industry is the phenomenon of pile run. Pile run refers to the sudden, uncontrolled freefall of a pile during installation, a phenomenon that can occur unexpectedly and have severe consequences (DNV, 2022).

Pile run events pose substantial risks to offshore operations, potentially causing equipment damage, project delays, and significant safety hazards. Current industry guidance documents, such as those from DNV, acknowledge this risk but provide limited methods for prediction. Traditional pile-driving analyses based on static soil resistance calculations often fail to anticipate such sudden events. Figure 1 provides a high-level summary of operation phases and associated risks that can contribute to pile run. There is presently an increased focus from industry on this phenomenon as demonstrated by paper submissions for 5th International Symposium on Frontiers in Offshore Geotechnics (held in June 2025) which included six entries related to pile run (Ghasemi et al, 2025; Kashichenula, 2025; Rosati et al, 2025; Senanayake et al, 2025; Vergote & Burgraeve, 2025; and Zhang et al, 2025).

Building on recent advancements in analytical modelling of rate-dependent soil resistance and experimental insights into excess pore pressure accumulation in transitional soils, this paper aims to develop, using advanced numerical analysis, a comprehensive, risk-focused framework for predicting offshore pile run initiation and progression under real-world installation scenarios.

2 PREVIOUS STUDIES INTO PILE RUN RISK

Pile-run incidents have been observed to occur more frequently in offshore wind farms, mainly because they are constructed in regions with limited prior offshore experience and where large pile diameters and hammer sizes are used. Hence, there has been an increased focus on the causes and prediction of pile run in recent times. Various authors have proposed and developed frameworks for analysis of pile run (Vergote et al., 2025; Zhang et al., 2025; Senanayake et al., 2025; Duffy et al., 2025). These developed frameworks consider static resistance, dynamic effects through consideration of the system's kinetic energy, and rate effects. The development and prediction of pile run have mainly been based on back analysis of driving data, which relies on Soil Resistance to Driving (SRD). However, the SRD methods do not capture the generation of excess pore water pressure due to hammer blows, leading to a reduction in driving resistance and potentially resulting in pile run. Rosati et al. (2025) tested the hypothesis that energy and blows impacting a pile will generate excess pore water pressures, leading to a gradual reduction in driving resistance, through an experimental program conducted on a geotechnical centrifuge. Preliminary experimental results showed that the accumulation of excess pore water pressure during consecutive blows decreased driving resistance.

This paper provides additional insight into pile run using advanced numerical modelling and analyses. Numerical dynamic finite element analyses (FEA) are carried out to provide insight into excess pore pressure generation and, hence, the reduction in SRD.

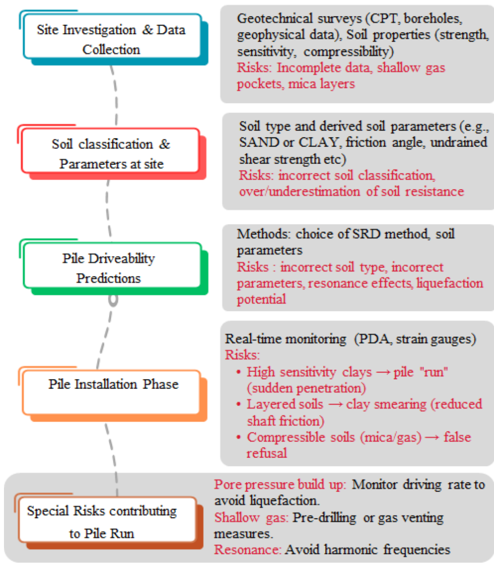

Figure 1. Summary of operations phases and associated risks that could contribute to pile run.

3 FUNDAMENTALS BEHIND PILE RUN

Figure 1 illustrates the potential risks that may contribute to pile runs. The key risks that may contribute to the occurrence of pile run are insufficient geotechnical characterisation and parameters, the adoption of an SRD methodology or a pile run estimation methodology that is not suitable for site-specific conditions, or poor pile-driving installation methodology.

Pile run is more likely in areas with weak or unconsolidated soils, such as soft clays or silts, where the soil is easily displaced. Therefore, geological drivers have the main impact on monopile installation, including:

- *Paleochannels and Subsurface Heterogeneity*

Paleochannels are ancient riverbeds infilled with heterogeneous sediments, which introduce abrupt variations in soil stiffness and strength. These features can trigger pile run, whether unexpected or anticipated, when soft deposits (e.g., organic-rich muds) are encountered, reducing shaft friction (LeBlanc et al., 2010).

- *Soil stratification and weak layers*

Weak interbeds (e.g., loose sands, sensitive clays) in stratified seabed profiles can cause sudden drops in driving resistance.

For example, silty clay layers will remould under cyclic loading, further diminishing shear strength (Jardine et al, 2005).

Local geotechnical modelling, integrating in situ Cone Penetration Test with pore water pressure (CPTu) data and laboratory shear tests, is required to forecast layer-specific resistance and maximise drivability (Achmus et al., 2009).

- *Soil Saturation and Pore Pressure Effects*

Several studies have reported on the generation of excess pore water pressure (PWPs) during pile driving. Pile installation using impact hammers affects the surrounding soil and induces large shear strains, leading to changes in the stress state and pore pressure response near the pile (Yazdani et al., 2020). Excessive pore pressure generation during dynamic pile driving diminishes effective stress, especially in low-permeability formations (e.g., silts, clays), resulting in temporary liquefaction and pile run (Randolph, 2003). The rate of dissipation of such pressures, dictated by soil consolidation characteristics, needs to be analysed to estimate re-stiffening after installation. Sophisticated finite-element (FE) analyses (e.g., PLAXIS 3D) can model pore pressure behaviour to guide installation procedures (Burd et al., 2020).

4 SRD ASSESSMENTS

4.1 *SRD assessment methodologies*

Several methods are available in the literature to assess SRD. These methods assess static soil resistance and are generally developed based on back-analysis of pile-driving data. The following Cone Penetration Test, CPT-based methods were reviewed and used to assess SRD, considering a fully coring pile.

- ***Alm and Hamre (1998, 2001):*** This methodology was developed considering CPT data as the primary input. It was initially developed in 1998 and updated in 2001, considering a larger database of driven piles. This methodology was developed based on pile-driving records from the North Sea. Pile diameters range between 1.83m and 2.74m. Friction fatigue in both sands and clays is used in assessing static resistance.
- ***Maynard et al. (2019):*** This methodology is a modification of the Alm and Hamre (2001) method, considering the driveability of monopiles. The database considered piles installed in varying soil conditions from the North Sea: quaternary deposits overlying cretaceous chalk, Eocene Thames London Clay and Paleogene deposits consisting of very stiff to hard clays, dense to very dense sands. The pile sizes considered ranged between 4.8m to 7.5m in diameter. Fitting parameters were derived based on the formulations presented by Alm and Hamre.
- ***Jones et al (2021):*** This methodology is a modification of the Alm and Hamre (2001) method. The database considers a wide range of soil conditions from normally consolidated clays offshore China to very dense sands and over-consolidated clays in the North Sea and mudstone in the Irish Sea. Pile diameters ranged between 0.66m and 6.5m. The key update in this method is the improved prediction of shaft friction for over-consolidated cohesive soils.
- ***MonoDrive (Stergiou et al., 2023):*** This methodology has been developed considering pile driving data from wind farms in the North and Irish Seas. Pile diameters considered ranged between 5.6m and 8.40m. The methodology considers CPT data. The methodology is a modification of the SRD methods developed by Byron et al. (2012), Schneider & Harmon (2010) and the Unified CPT SRD method (Lehane et al, 2022). Fitting parameters were calibrated and optimised against a database and used in the SRD method.

4.2 *Comparison of SRD by different methods*

SRDs were calculated using different methods for a typical offshore CPT profile with pile-run risk, as shown in Figure 4. Figure 2 presents the SRDs (Best Estimate - BE) for all four methodologies discussed in the previous section for the CPT profile provided in Figure 4. The above methods for estimating SRD should be used with caution, as they depend on the database from which they were developed. Maynard et al. (2019) and Stergiou et al. (2023) state that the databases used to develop SRD methods should be updated to improve the accuracy and applicability of SRD estimation. In the current study, SRD following Maynard et al. (2019) will be used, as it was developed for large-diameter piles and provides the lowest SRD. Thus, for pile sun assessment, it is conservative to use this SRD.

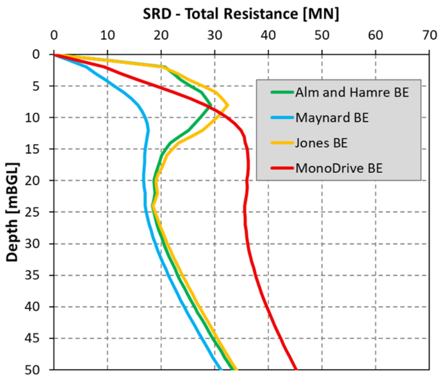

Figure 2. SRD results were determined using four SRD methods: Alm and Hamre (2001), Maynard et al. (2019), Jones et al (2021), and MonoDrive (Stergiou et al., 2023).

5 NUMERICAL ASSESSMENT

Pile driving is a dynamic process that causes vibrations in the surrounding soil. It is expected that the soil in the vicinity of the pile will experience excess pore pressures due to dynamic loading (Senanayake et al., 2025; Vergote & Burgraeve, 2025; Rosati et al., 2025; Plaxis, 2021). Numerical dynamic finite element (FE) analyses were conducted to investigate the generation of excess pore pressures below the pile toe under various scenarios. Table 1 presents a summary of the Plaxis models analysed.

5.1 *Pile geometry and hammer configuration weights*

The monopile considered was a hollow steel pile with an outer diameter D = 8.0m, a wall thickness t = 0.08m, a length L = 65m, and an embedment depth of 9 m. The monopile's total self-weight is circa 10 MN. Hydrohammer IHC S-2000 was considered in this analysis. The total weight of the hammer (including ancillary items) of 550 tonnes (circa 5.5MN) has been considered in the current assessments.

5.2 *Finite Element Model (PLAXIS)*

A two-dimensional axisymmetric fully coupled, nonlinear dynamic FE analysis was carried out to understand the excess pore pressure generation due to pile driving. The water table was set at ground level. Plaxis 2D Ultimate software and the UBC3D-PLM constitutive model were used to model the dynamic behaviour of the soil under pile driving loading. UBC3D-PLM is an effective stress-elastoplastic model capable of simulating the liquefaction of sandy soil under dynamic loading conditions (Chakraborty & Sawant, 2022). Further details about the UBC3D-PLM model can be found in the work of Petalas & Galavi (2013).

The mesh density was determined using Equation (1)

$$Average\ Element\ Size = V_{s,min} / 8 f_{max} \qquad (1)$$

where $V_{s,min}$ is the lowest shear wave velocity, and f_{max} is the highest frequency of the input dynamic load.

A volume cluster with linearly elastic non-porous material behaviour is selected to model the monopile, with a unit weight γ of 77kN/m^3, a Young's modulus E of 210 GPa, and a Poisson's ratio ν of 0.1 (Plaxis, 2021). Interface elements are placed on both the inner and outer sides of the pile to model the interaction between the pile and the soil, with a coefficient of reduction of the shear strength equal to R_{inter} = 0.67 along the shaft (Sun et al., 2017).

The FE model extended laterally from the axisymmetric axis by 50m and vertically by 100m, corresponding to $6.25 \times D$ (where D is the pile diameter) and $1.5 \times L$ (where L is the pile length), approximately, eliminating the effect that could be developed as a result of the boundaries, such as wave reflections (Figure 3). These model dimensions were determined from a preliminary sensitivity analysis that showed the boundaries did not affect the FEA results. Furthermore, the model dimensions agree with previous studies performed on caisson foundations and onshore wind turbines under seismic loading (Gaudio et al., 2016; Gaudio et al., 2023; Zhang & Zhu, 2022). To avoid spurious wave reflections within the soil domain, viscous boundaries were used to simulate the far-field behaviour by absorbing dynamic loading-induced stress increments. The UBC3D-PLM model has advantages and limitations in its use and applicability (Petalas & Galavi, 2013). Although the UBC3D-PLM model is adequate for capturing the liquefaction behaviour of sand layers, it is insufficient to estimate initial stress conditions. Therefore, the Hardening Soil model with small-strain stiffness (HS-small) was used to accurately model the initial stress conditions.

The numerical analyses for all the plaxis models in Table 1 were carried out in three stages: The first stage, the initial stress field was established using K_0 procedure and HS-small model. In the second stage, monopile was wished in place at 9m below ground level (bgl) as at this depth pile plus hammer weight (i.e. 15.5MN) is in equilibrium with soil resistance in driving (SRD) as shown in Figure 4. In the third stage, "dynamic with consolidation analysis" in a coupled manner using two permeability values k_1=1x10^{-5} m/s (coarse sand) and k_2=1x10^{-7} m/s (fine sand-silt mixture) was performed by replacing the HS-small model with the UBC-PLM model. The drainage type used was Undrained A.

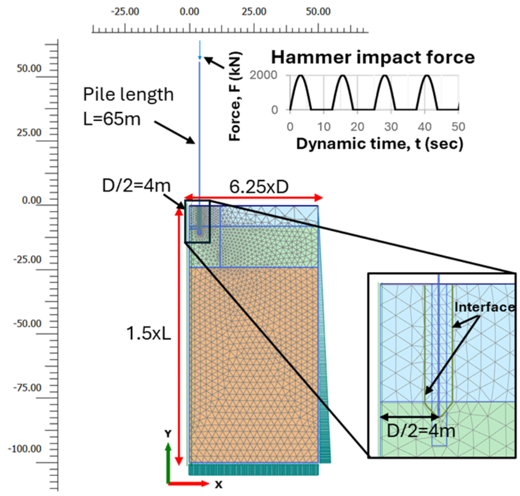

Figure 3. 2D axisymmetric finite element model used in the study.

Table 1. Summary of Plaxis models analysed.

Plaxis model	Energy, E_r (kJ)	Amplitude A (kN/m^2)	Rate (Blows /min)	f (Hz)	Blows, N
1a	200	2010	10	0.17	125
1c	200	2010	35	0.58	125
2a	2000	20095	10	0.17	125
2c	2000	20095	35	0.58	125
3a	500	5024	35	0.58	125
3b	1000	10048	35	0.58	125
3c	1000	10048	10	0.17	125

5.2.1 *Soil profile and constitutive model soil parameters*

The soil profile used for this study was developed based on a typical offshore CPT profile, as shown in Figure 4. Brinkgreve et al. (2010) proposed empirical formulas to determine HS-Small parameters. All formulas are expressed based on relative density (D_r). The UBC3D-PLM model has 15 parameters, and the model parameters were determined using corrected SPT blow counts $(N_1)_{60}$, as proposed by Beaty & Byrne (2011; Arboleda-Monsalve & Nguyen, 2016; Galavi, V., & Tehrani, 2017). The relative density, D_r, was selected using the empirical correlation proposed by Jamiolkowski et al. (2003). Table 2 summarises the soil profile and key soil parameters used in this study.

In Plaxis 2D, both viscous (radiation) damping and hysteretic (material) damping are accounted for. The former is considered in the analysis using Rayleigh damping. In the current study, a damping ratio value ξ (typically chosen between 0.5-2% as recommended from Plaxis 2D) was assumed, and the target frequencies ($f_1 = \frac{V_s}{4H}$ and f_2 is the closest odd number given by the ratio of the dynamic load predominant frequency and f_1) were obtained employing the procedure proposed by Hudson et al. (1994). Rayleigh damping coefficients α of 3.685x10^{-2} and β of 9.57x10^{-4} associated with a small damping ratio ξ of 1% were considered in this study.

5.2.2 *Hammer impact load*

The hammer impact (i.e. force time history) at the top of the monopile was simulated using a line load with assigned dynamic multipliers having the shape of a half-sine wave, as shown in Figure 3 using Equation (2).

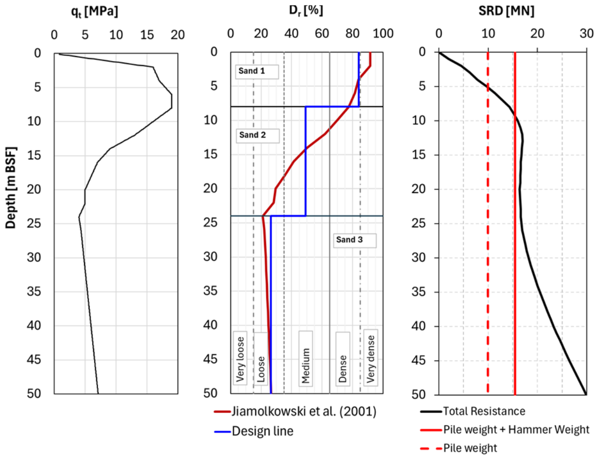

Figure 4. A typical offshore CPT profile, relative density profile, and SRD calculated using the modified Alm and Hamre (2001) method (Maynard et al., 2019).

Table 2. Soil profile and key soil parameters.

Layer	Depth below Seabed Level (m bsl) Top	Depth below Seabed Level (m bsl) Bottom	Average q_t (MPa)	γ (kN/m³)	D_r (%)	$(N_1)_{60}$ (-)
Sand 01	0	8	15.4	19	84	31
Sand 02	8	24	9.1	19	49	15
Sand 03	24	75	7.2	19	27	10

$$F = A \times \sin[(2\pi f) \times t] \tag{2}$$

where F is the instantaneous force at time t, A is the amplitude of the force, f is the frequency (i.e. blow rate) and t is the dynamic time.

The minimum and maximum blow energy (i.e. kinetic energy E_r) of the IHC S-2000 hammer is 200kNm and 2000 kNm, and the maximum blow rate is 35blows/min (i.e. f=0.58Hz) according to the hammer specification. When the hammer hits the pile, it decelerates rapidly over a very short time. Using the work-energy principle given in Equation (3) and assuming a deceleration distance d of 50mm, the hammer blow energy is converted to the amplitude of the hammer force amplitude of A.

$$A = \frac{E_r}{A_{pile}\ x\ d} \tag{3}$$

where A is the amplitude of hammer force (in kN/m²), E_r is the kinetic or blow energy (in kNm), and d is the deceleration distance in m (i.e. distance over which the hammer decelerates), and A_{pile} is the pile area (in m²). Table 1 summarises the Plaxis input parameters for each model.

The force time history at the pile head was simulated in Plaxis 2D as a half-sine wave (Figure 3) with amplitude A ranging between 2010kN/m² and 20095kN/m² corresponding to minimum and maximum hammer energy. The dynamic calculations were conducted over the time interval, Δt, that is equal to the measured time of impact during the field test. This time interval was subdivided into a maximum number of steps, m, and several sub-steps, n. The parameters m and n are used to discretise the dynamic time interval into the most suitable number of time steps, ensuring that the dynamic loading is adequately covered. A maximum number of blows N of 125 (refusal based on ISO 19901-4:2016) and blow rate ranging between 5-35blow/min (i.e. f=0.08-0.58Hz) is considered in this study. Therefore, the duration of the hammer force time history ranges between 215.5sec to 1562.5sec, depending on the selected blow rate. In Plaxis 2D, numerous calculation steps were stored to allow extracting the results for intermediate blow number (e.g. N=1, 5, 10, 20, 50, and 125).

6 SRD CALCULATION FROM NUMERICAL RESULTS

Soil Resistance to Driving (SRD) was calculated using Maynard et al. (2019) and CPT data (Figure 4). The method is based on offshore piling data consisting of 202 pile drivability records from three sites with varying soil conditions. The Maynard et al. (2019) method is based on CPT data with no limits to either unit skin friction or end resistance values. SRD formulations are provided in Maynard et al. (2019). Using a typical offshore cone penetration test (CPT) data, SRD vs depth profile is estimated as shown in Figure 4. One of the key input parameters for Maynard et al. (2019) method is the effective overburden stress. As noted above, dynamic pile driving generates excess pore water pressures (PWP), reducing the effective stress, particularly in soils with low permeability. For the SRD calculations, only the reduction in effective stress due to excess pore was considered, and cone resistance q_t, was assumed to remain unchanged. In reality, the cone resistance q_t would also reduce and hence lead to further SRD reductions. This needs project-specific information and advanced assessments, which are beyond the scope of this paper. The reduced effective stresses were calculated based on pore pressure ratio $r_{u,\sigma v'}$, which were extracted from the Plaxis numerical model at the pile-soil interface and utilised in Maynard et al. (2019) method to assess the effect of the following parameters on SRD profile:

- Hammer energy, E_r; and
- Number of blows, N
- Permeability of seabed soil, k

7 RESULTS & DISCUSSION

The results from numerical analyses indicate that variations in energy input, blow rate, and number of blows significantly influence Soil Resistance to Driving (SRD), with higher energy and number of blows generally leading to increased soil disturbance and excess pore pressures, and therefore a reduced SRD-depth profile. The SRD results presented below in section 7.1 and 7.2 correspond to k_2=1x10^{-7} m/s(fine sand-silt mixture).

7.1 *Effect of hammer energy, E_r*

Figure 5 illustrates the effect of hammer energy (E_r) on the SRD profile. The results indicate the following:

- Hammer energy has a significant impact on SRD.
- At high blow rates and low numbers of blows, SRD can decrease by a maximum of 29%, with an average reduction of approximately 6.5%.
- At high blow rates and a high number of blows, SRD can decrease by a maximum of 62%, with an average decrease of approximately 29%.
- When using high hammer energy (e.g., 2000 kJ) combined with a high number of blows, a maximum SRD reduction of 62% is observed, primarily due to the liquefaction of deeper sand layers (specifically, Layer Sand 03).

7.2 *Effect of number of blows, N*

The influence of the number of blows (N) on the SRD profile is illustrated in Figure 6. The results reveal the following trends:

- For low hammer energy (200 kJ), SRD can decrease by a maximum of 21%, with an average reduction of approximately 2.5%.

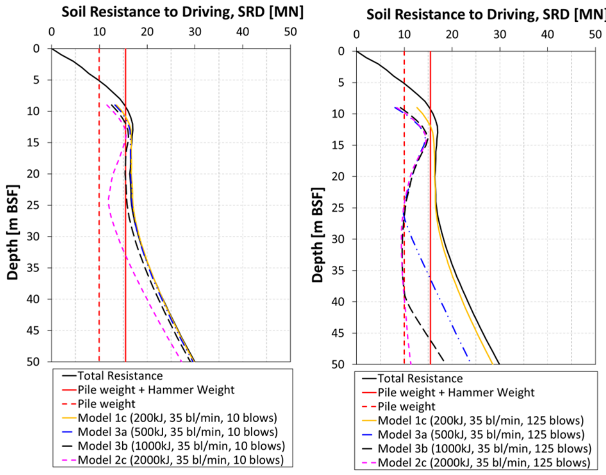

Figure 5. Effect of hammer energy (E_r) on SRD-depth profile.

- For high hammer energy (2000 kJ), a more substantial SRD reduction is observed, ranging from 6% to 62%, with an average of approximately 30%.
- SRD reduction appears largely independent of blow rate, as the average difference across varying blow rates is only about 0.3% and 1.2%, for low (200kJ) and high (2000kJ) hammer energy.

7.3 *Effect of soil permeability, k*

Figure 7 presents the influence of soil permeability (specifically, k1=1x10-5 m/s and k2=1x10-7 m/s) on the PWP generated at the pile toe during the first 6s (rate of 10 blows per min was analysed). The analyses considered 3 hammer energies (E_r), 200 kJ, 1000 kJ, and 2000 kJ respectively. The results provide the following insight:

- As the hammer energy increases, the generation of excess pore water pressure (PWP) exhibits a linear trend.
- As expected, sand with higher hydraulic conductivity (k_1=1x10^{-5} m/s) generates lower excess PWP compared to sand with low hydraulic conductivity (k_2=1x10^{-7} m/s).

Figure 8 presents the pore pressure ratio generated after 10 blows along the depth at the pile wall location for two different hydraulic conductivities. It is evident that lower hydraulic conductivity results in temporary liquefaction at certain depths (i.e. pore pressure ratio $r_u > 0.8$, Olson et al., 2020) as shown in Figure 8. This highlights the importance of temporary liquefaction which can trigger the pile run.

8 CONCLUSIONS

This paper examined the key factors contributing to pile run by numerical analysis. Based on the results presented in this study, the following conclusions can be drawn:

- A two-dimensional axisymmetric fully coupled, nonlinear dynamic FE analysis using UBC3D-PLM constitutive model, can help in pile run risk prediction by capturing excess pore pressure generation due to dynamic loading.
- It is important to note that SRD calculations (Figure 2) do not account for excess pore pressures, due to dynamic loading, which can trigger pile run.
- Excess pore pressure builds up during impact driving depends on soil permeability and hammer energy.
- An improved SRD prediction method can be achieved by integrating CPT-based analytical approaches (e.g. Maynard et al., 2019) with numerical model outputs, incorporating dynamic effects and excess PWP to better reflect real-world installation conditions.

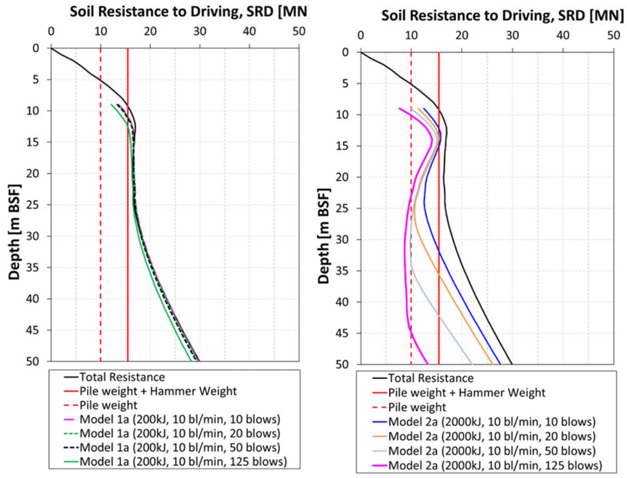

Figure 6. Effect of number of blows on SRD results for low blow rate 10bl/min.

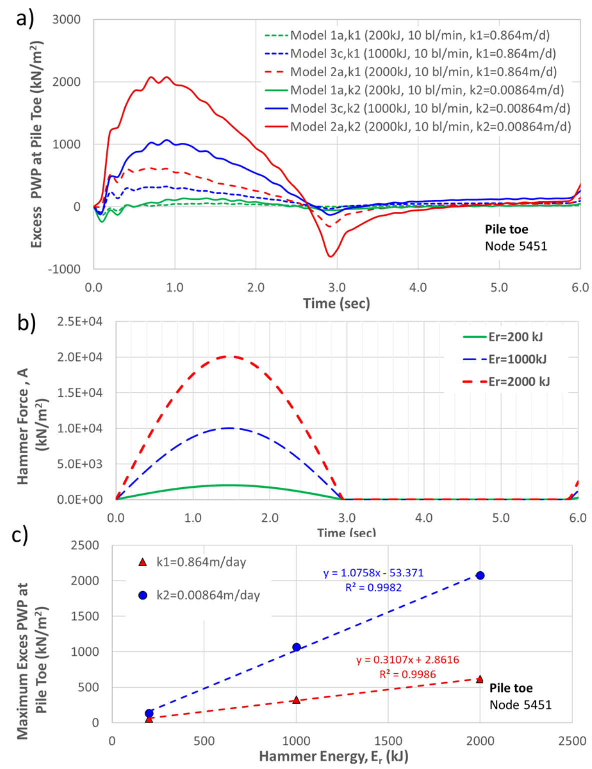

Figure 7. Influence of soil permeability and hammer energy on the excess PWP generated at the pile toe during a single hammer blow.

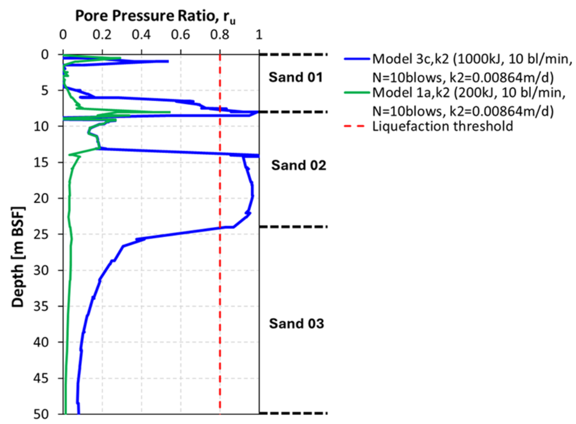

Figure 8. Effect of hammer energy on excess pore pressure ratio, r_u, after 10 blows at rate of 10bl/min, low permeability (k_2=1x10^{-7} m/s).

9 REFERENCES

Achmus, M., Kuo, Y.-S., and Abdel-Rahman, K. 2009. 'Behavior of monopile foundations under cyclic lateral load', Computers and Geotechnics, 36(5), pp. 725–735.

Alm, T. and Hamre, L. (1998). Soil Model for Driveability Predictions. OTC 8835, Offshore Technology Conference, No. OTC 8835, 13.

Alm, T., & Hamre, L. (2001). Soil model for pile driveability predictions based on CPT interpretations. In International Conference on soil mechanics and geotechnical engineering (pp. 1297-1302).

API (1981) Recommended Practice for Planning, Design and Constructing Offshore Platforms, API RP 2A, 12th Edition.

Arboleda-Monsalve, L. G., & Nguyen, H. (2016). Simulation of Liquefaction-induced Damage of the Port pf Long Beach Using the UBC3D-PLM Model (No. CA16-2933).

Beaty, M.H. & Byrne, P.M. 2011. UBCSAND constitutive model. Version 904aR. Documentation report: UBCSAND constitutive model on Itasca UDM website.

Brinkgreve, R.B.J., Engin, E. & Engin H.K. 2010. Validation of empirical formulas to derive model parameters for sands, NUMGE conference, CRC Press, Trondheim, Norway.

Burd, H. J. et al. 2020. PISA design model for monopiles for offshore wind turbines: application to a marine sand. Géotechnique 70, No. 11, 1048–1066.

Byrne, T., Doherty, P, Gavin K., and Overy R. (2012). Comparison of pile driveability methods in North Sea sand. Offshore Site Investigation and Geotechnics: Integrated Technologies - Present and Future, 12-14 September, London, UK

Byron et al. (2012), Schneider & Harmon (2010) and Unified CPT SRD method (NGI, 2019).

Chakraborty, A., & Sawant, V. A. (2022). Numerical simulation of earthen embankment resting on liquefiable soil and remediation using stone columns. International Journal of Geomechanics, 22(11), 04022205.

DNV.2022. DNV-RP-C212: Offshore Soil Mechanics and Geotechnical Engineering.

Galavi, V., & Tehrani, F. S. (2017). Empirical and numerical analyses of soil liquefaction around buried offshore pipelines. *ISSMGE, PBD-III Vancouver, Earthquake Geotechnical Engineering, paper*, *475*.

Gaudio D., Seong J., Haigh S., Viggiani G. M. B., Madabhushi G. S. P., Shrivatsava R., Veluvolu R., Padhy P. (2023). Boundary effects on dynamic centrifuge modelling of onshore wind turbines on liquefiable soils. International Journal of Physical Modelling in Geotechnics, ICE Publishing, 23(1): 16-34, ISSN: 1346-213X, https://doi.org/10.1680/jphmg.21.00085

Gaudio, D., Rampello, S. (2016). Dynamic soil-structure interaction of bridge-pier caisson foundations. In Geotechnical engineering in multidisciplinary research: from microscale to regional scale CNRIG2016. VI Italian Conf. of Researchers in Geotechnical Engineering, Procedia Engineering, Elsevier, 158: 146-151, https://doi.org/10.1016/j.proeng.2016.08.420

Ghasemi, P., et al. 2025. Adjustment of an SRD model for the self-weight penetration and pile run analysis of monopiles in North Sea soil condition. Proceedings of ISFOG 2025, 5th INTERNATIONAL SYMPOSIUM ON FRONTIERS IN OFFSHORE GEOTECHNICS, Nantes, France, June 9-13, 2025

GWEC. 2025. Global Wind Report 2025.

Hudson, M, Idriss, IM, and Beikae, M. 1994., QUAD4M - A computer program to evaluate the seismic response of soil structures using finite element procedures and incorporating a compliant base., in, Center for Geotechnical Modeling, Department of Civil and Environmental Engineering, University of California, Davis, CA., Davis, CA, 1994.

ISO (2016). ISO 19901-4:2016 – Petroleum and natural gas industries — Specific requirements for offshore structures — Part 4: Geotechnical and foundation design considerations. 2nd ed. International Organization for Standardization.

Jamiolkowski, M., Lo Presti, D.C.F., and Manassero, M. 2003. Evaluation of relative density and shear strength of sands from cone penetration test (CPT) and flat dilatometer (DMT). In Soil behaviour and soft ground construction, 119, pp. 201-238.

Jardine, Richard & Merritt, Andrew & Schroeder, Felix. 2015. The ICP Design Method and Application to a North Sea Offshore Wind Farm. Geotechnical Special Publication. 247-256. 10.1061/9780784479087.025.

Jones, L., Rattley, M. and Mancaeau, S (2021) A CPT Based Soil Resistance to Driving (SRD) Method for Offshore Pile Driveability Analyses. Proceedings of the piling Conference

Kashichenula, K., Sudhakaran, K., and Maghsodi, S. 2025. Performance of different soil resistance models to assess the pile runs during offshore pile driving. Proceedings of ISFOG 2025, 5th INTERNATIONAL SYMPOSIUM ON FRONTIERS IN OFFSHORE GEOTECHNICS, Nantes, France, June 9-13, 2025

LeBlanc, C., Houlsby, G.T. & Byrne, B.W. 2010. Response of Rigid Piles in Sand to Long-Term Cyclic Lateral Loading. Géotechnique, 60(2), pp. 79–90.

Lehane et al (2022). Application of the Unified CPT method to assess the Driving Resistance of Pipe Piles in Sand. 11th International Stress Wave Conference, Rotterdam, the Netherlands

Liqiang Sun, Yandi Wang, Wei Guo, Shuwang Yan, Jian Chu & Xiaoqiang Liu (2017): Case study on pile running during the driving process of large-diameter pipe piles, Marine Georesources & Geotechnology, DOI: 10.1080/1064119X.2017.1386742.

Maynard W. Alice, Hamre Liv, Butterworth Daniel and Davison Fred (2019). Improved Pile Installation Predictions for Monopiles, 10th International Conference on Stress Wave Theory and Testing Methods for Deep Foundations.

Olson, S. M., Mei, X., & Hashash, Y. M. (2020). Nonlinear site response analysis with pore-water pressure generation for liquefaction triggering evaluation. Journal of Geotechnical and Geoenvironmental Engineering, 146(2), 04019128.

Petalas, A., and Galavi, V. (2013). Plaxis Liquefaction Model UBC3D-PLM

Plaxis 2D Tutorial Manual. 2021. Tutorial 16 - Pile driving (ULT).

Randolph, M.F. 2003. Science and empiricism in pile foundation design', Géotechnique, 53(10), pp. 847–875.

Rosati, A., et al. 2025. Centrifuge tests to investigate pile run risk in transitional soils. Proceedings of ISFOG 2025, 5th INTERNATIONAL SYMPOSIUM ON FRONTIERS IN OFFSHORE GEOTECHNICS, Nantes, France, June 9-13, 2025

Schneider, J.A., Hamon, I.A. (2010). Analyzing Drivability of Open Ended Piles in Very Dense Sands. The Journal of the Deep Foundations Institute

Semple, R.M and Gemeinhardt, J.P. (1981) Stress History Approach to Analysis of Soil Resistance to Pile Driving. Proceedings of the 13th Offshore Technology Conference, Houston, Texas.

Senanayake, A., et al. 2025. A CPT-based, critical-state approach for the analysis of pile run during driving operations. Proceedings of ISFOG 2025, 5th INTERNATIONAL SYMPOSIUM ON FRONTIERS IN OFFSHORE GEOTECHNICS, Nantes, France, June 9-13, 2025.

Stergiou, T., Perikleous, G. & Meissl, S. (2023) MonoDrive: A novel SRD methodology for offshore wind monopile foundations developed based on an extensive driveability database. Conference: 9th International SUT OSIG Conference "Innovative Geotechnologies for Energy Transition" At: London, UK. DOI:10.3723/CBWP3728

Vergote, T., and Burgraeve, A. 2025. A framework for analysis of pile run. Proceedings of ISFOG 2025, 5th INTERNATIONAL SYMPOSIUM ON FRONTIERS IN OFFSHORE GEOTECHNICS, Nantes, France, June 9-13, 2025.

Yazdani E, Wang J, Evans TM, Case study of a driven pile foundation in diatomaceous soil. II: Pile installation, dynamic analysis, and pore pressure generation, *Journal of Rock Mechanics and Geotechnical Engineering*, https://doi.org/10.1016/j.jrmge. 2020.10.005.

Zhang, J., & Zhu, S. Y. (2022). Dynamic responses of monopile supported wind turbines considering soil liquefaction. The 2022 World Congress on Advances in Civil, Environmental, & Materials Research (ACEM22) 16-19, August 2022, GECE, Seoul, Korea

Zhang, S., et al. 2025. A Novel Driveability Prediction Method for Continuous Impact Driving and Monopile Run. Proceedings of ISFOG 2025, 5th INTERNATIONAL SYMPOSIUM ON FRONTIERS IN OFFSHORE GEOTECHNICS, Nantes, France, June 9-13, 2025.